

# RADIO FREQUENCY QUADRUPOLE SURROGATE FIELD MODELS BASED ON 3D ELECTROMAGNETIC FIELD SIMULATION RESULTS\*

T. Roggen<sup>1,2</sup>, B. Masschaele<sup>1,3</sup>, H. De Gersem<sup>1,4</sup>, W. Ackermann<sup>4</sup>, S. Franke<sup>4</sup>, T. Weiland<sup>4</sup>  
<sup>1</sup>KU Leuven Kulak, WPSP, Belgium; <sup>2</sup>CERN, BE/RF, Switzerland;  
<sup>3</sup>Ghent University, Belgium; <sup>4</sup>TU Darmstadt, TEMF, Germany

## Abstract

Surrogate field models for the different sections of a Radio Frequency Quadrupole (RFQ) are developed, identified on the basis of finite element (FE) simulation and embedded in a moment method beam dynamics simulation code. The models are validated for both theoretical and realistic RFQ designs.

## INTRODUCTION

An RFQ is a low-velocity, high-current accelerator component that accelerates a DC particle beam ( $p^+$  to U), directly from the source, from several keV/nucleon to about  $2q/A_{\text{ION}}$  [MeV/nucleon], with  $A_{\text{ION}}$  the ion mass in amu. Two main RFQ types exist: a four-vane [1, 2] and a four-rod type [3], differing mainly in the RF field induction process. An RF source applies an alternating, focussing quadrupole electric field between the four rods. An accelerating field component is present due to a geometrical modulation of the rod along the beam axis. Figure 1 shows the input radial matcher (RM) (1) which adiabatically matches the DC-beam to the transverse electric focussing field. In the shaper section (3), coupled smoothly to (1) by an input transition cell (TC) (2), the bunching of the DC-beam is initiated. The gentle buncher section (4) continues the bunching adiabatically, until the beam is appropriately bunched. The final RFQ section, the accelerator (5), provides a longitudinal acceleration to the bunches, while the focussing component continues to maintain transverse stability. An output RM (7), coupled smoothly to the last accelerating cell by an output TC (6), ensures distortion-free decoupling of the bunches from the electromagnetic fields. The velocity-independent electric focussing and adiabatic bunching results in compact bunches and nearly 100 % capture and transmission efficiency.

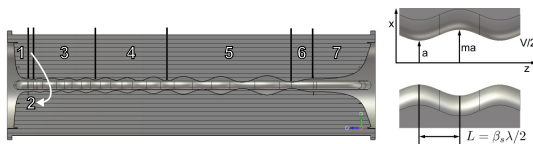


Figure 1: Longitudinal cross-section of an exemplary four-vane RFQ: Input radial matcher (RM) (1), input transition cell (TC) (2), shaper section (3), gentle buncher (4), accelerator section (5), output TC (6), output RM (7); RFQ rod tip geometry.

\* This research is funded by grant “KUL 3E100118” “Electromagnetic Field Simulation for Future Particle Accelerators”, the MAX project FP7-Euratom No. 269565 and the Belgian Nuclear Research Centre (SCK-CEN).

The RFQ is embedded as a beam line element in a Vlasov based moment method beam dynamics code. The particle beam is represented by a particle density function  $f(\mathbf{r}, \mathbf{p}, \tau)$  with  $\mathbf{r}$  the spatial coordinate,  $\mathbf{p}$  the normalised momentum,  $\tau = ct$  the equivalent time,  $c$  the velocity of light and time  $t$ .  $f(\mathbf{r}, \mathbf{p}, \tau)$  is tracked through the different particle accelerator components, with their individual characteristic electromagnetic fields exerting a force  $\mathbf{F}$  on the particles, by solving the Vlasov equation [4, 5]

$$\frac{\partial f}{\partial \tau} + \frac{\partial f}{\partial \mathbf{r}} \cdot \frac{\mathbf{p}}{\gamma} + \frac{\partial f}{\partial \mathbf{p}} \cdot \frac{\mathbf{F}}{m_0 c^2} = 0, \quad (1)$$

with  $\gamma$  the Lorentz factor,  $m_0$  the rest mass. In the implementation called V-Code [6], the Vlasov equation is discretised in phase space by the moment method [7] and in time by a fourth-order Runge-Kutta-Fehlberg method [6, 8, 9]. V-Code is extended to allow simulations of particle accelerators incorporating RFQs.

## SCALAR POTENTIAL FUNCTION

A multipole expansion of the electromagnetic field distribution can be derived from field data of finite element (FE) or finite difference time domain (FDTD) simulation results (e.g. from CST STUDIO SUITE® [10]). The RFQ’s electromagnetic field distribution between the rods can be determined on a cell-by-cell basis using a quasi-static approximation [11, 12] based on the scalar potential function  $U(r, \theta, z, t)$  [1]:

$$U(r, \theta, z, t) = \sin(\omega t + \phi) \left[ \sum_{p=0}^{\infty} A_{0,2p+1} r^{2(2p+1)} \cos(2(2p+1)\theta) + \sum_{n=1}^{\infty} \sum_{s=0}^{\infty} A_{n,s} I_{2s}(k_{\text{CELL}} nr) \cos(2s\theta) \cos(k_{\text{CELL}} nz) \right], \quad (2)$$

with cell length  $L$  (Fig. 1),  $(r, \theta, z)$  the cylindrical coordinate system,  $t$  the time,  $\omega$  the RF angular frequency,  $\phi$  the initial phase shift and  $p, s$  and  $n$  multipole component indices with restriction  $n+s = 2p+1$ .  $I_{2s}$  is the modified Bessel function,  $A_{0,2p+1}$  and  $A_{n,s}$  are pole tip geometry dependent multipole coefficients in function of the modulation parameter  $m(z)$ , the minimum aperture  $a$ , the rod potential difference  $V_0$ ,  $k_{\text{CELL}} = 2\pi/2L$ ,  $2L = \beta_s \lambda$  the rod modulation period,  $\beta_s$  the synchronous particle velocity and  $\lambda$  the wave length.  $\mathbf{E} = -\nabla U$  is the associated electric field strength.

Similar expressions can be found for the RM (Eq. 3) and the TC (Eq. 4). The RM ranges between  $z = -L_{\text{RM}}$  and  $z = 0$ , and  $k_{\text{RM}} = \pi/2L_{\text{RM}}$ . For the TC  $k_{\text{TC}} = \pi/2L_{\text{TC}}$  and  $L_{\text{TC}}$

Content from this work may be used under the terms of the CC BY 3.0 licence (© 2014). Any distribution of this work must maintain attribution to the author(s), title of the work, publisher, and DOI.

is the length of the TC [13].

$$U(r, \theta, z, t) = \sin(\omega t + \phi) \left[ \sum_{n=0}^3 A_n \cos(2n\theta) \left( I_{2n}(k_{RM}r) \cos(k_{RM}z) + \frac{I_{2n}(3k_{RM}r) \cos(3k_{RM}z)}{3^{2n+1}} \right) \right] \quad (3)$$

$$U(r, \theta, z, t) = \sin(\omega t + \phi) [A_{0,0}r^2 \cos(2\theta) \pm A_{1,0}I_0(k_{TC}r) \cos(k_{TC}z) \pm A_{3,0}I_0(3k_{TC}r) \cos(3k_{TC}z)] \quad (4)$$

## SURROGATE FIELD MODEL

### Shaper, Gentle Buncher and Accelerator Section

Equation 2 assumes an idealised RFQ geometry and has limited value in practice. Instead, an identification of the multipole coefficients on a cell-by-cell basis by applying a nonlinear regression to the field data of a 3D FE/FDTD simulation of the RFQ, expanded with correction terms, allows to reconstruct an accurate multipole RFQ surrogate field model. An eight-term potential function with multipole coefficients is already found to be accurate in [14]. A further refinement with additional polynomial correction terms improves accuracy significantly [15]. The surrogate field models were validated for theoretical 3D RFQ models, with and without noise added to the data set. As a criterion, the residuals of the regression model ( $\delta_{res,i} = y_i - f_i$ , with  $\delta_{res,i}$  the residual for data point  $i$ , data point value  $y_i$  and regression function value  $f_i$ ). Table 1 summarises the residual interval for both data sets. The generated surrogate model for the noiseless data represents the 3D data set nearly perfectly. The surrogate model with correction terms generated with the noisy data set is able to represent all noisy (*measured*) and noiseless (*true*) data points with a maximum error of respectively 4.8% and 0.2%. Validation for the MYRRHA

Table 1:  $\delta_{res,i}$  for the eight-term and corrected eight-term RFQ model obtained by identification collocation for a noiseless and a noisy 3D scalar potential data set.

Data set	Eight-term $\delta_{res,i}$ [%]	Corr. eight-term $\delta_{res,i}$ [%]
Noiseless	$-0.2 < \delta_{res,i} < 0.3$	$-4.7e^{-3} < \delta_{res,i} < 4.7e^{-3}$
Noisy	$-4.7 < \delta_{res,i} < 4.9$	$-4.8 < \delta_{res,i} < 4.7$
Noiseless, noisy coeff. fit	$-0.4 < \delta_{res,i} < 0.6$	$-0.2 < \delta_{res,i} < 0.2$

RFQ [16] ( $\Delta U = \pm 20$  kV) results in a confidence interval of maximum  $\pm 1.3$  % without and maximum  $\pm 0.9$  % with correction terms added to the surrogate model (Fig. 2). The contribution of the correction terms is understood better when one investigates individual cells: Fig. 3 visualises  $\delta_{res,i}(z)$ , with  $z = 0$  for the cell's centre. The cells clearly have a distribution of  $\delta_{res,i}$  in function of  $z$ , enabling the corrected eight-term to not only reduce the confidence interval but also improve the potential approximation significantly in the region of the cell entrance and exit, contributing to accurate beam dynamics simulations for the RFQ in V-Code. Note that the corrected eight-term model may be introduced in non-Vlasov based beam dynamics codes as well.

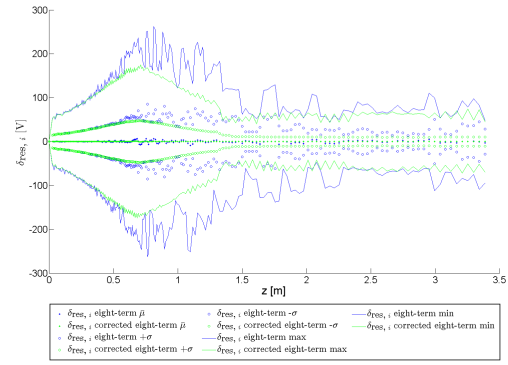


Figure 2: MYRRHA RFQ: Mean  $\delta_{res,i}$   $\pm \sigma$  interval and max/min  $\delta_{res,i}(z_{cell\ centre})$  for the eight-term and corrected eight-term identification collocation method.

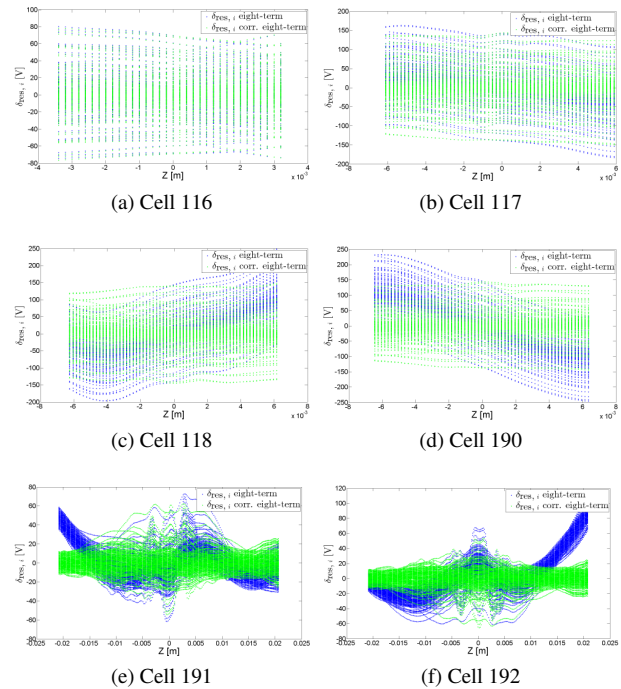


Figure 3: MYRRHA RFQ: For different cells  $\delta_{res,i}$  for the eight-term RFQ and corrected eight-term RFQ.

### Radial Matcher

The identification collocation method for the RM model determines the multipole coefficients of Eq. 3. It is applicable to both input and output RMs. Additional correction terms do not contribute to more accurate field reconstruction and are omitted. Validation results for the theoretical 3D RFQ models are summarised in Table 2. The generated surrogate model for the noiseless data represents the 3D data set nearly perfectly. The noisy and noiseless data points are represented with a maximum error of respectively 7.7% and 0.3%. Application to the MYRRHA output RM yields values for  $\delta_{res,i}$  within a confidence intervals of maximum  $\pm 2.0$  % (Fig. 4). Similar results are found for the MYRRHA input RM. The accuracy of the generated model

is near the edge of usability, caused by two effects in the realistic model: The RM ends do not extend to infinity and the milled MYRRHA RFQ rod surface deviates from the ideal model. A compatibility verification of the surrogate field model with the true RFQ RM's rod structure is therefore always mandatory.

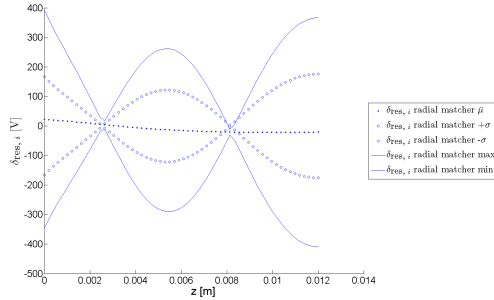


Figure 4: MYRRHA RFQ: Mean  $\delta_{res,i}(z_{cell\ centre})$ ,  $\pm\sigma$  interval and max/min  $\delta_{res,i}(z_{cell\ centre})$  for the RM identification collocation method applied to the output RM.

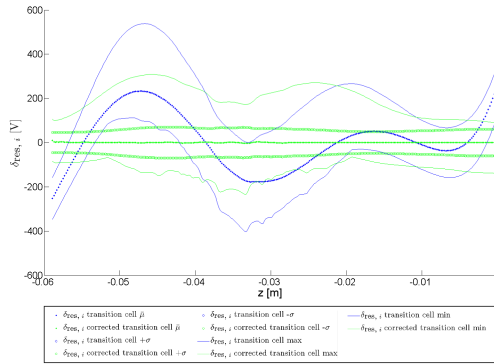


Figure 5: MYRRHA RFQ: Mean  $\delta_{res,i}(z_{cell\ centre})$ ,  $\pm\sigma$  interval and max/min  $\delta_{res,i}(z_{cell\ centre})$  for the TC and corrected TC identification collocation method applied to the output TC.

### Transition Cell

The identification collocation method for the TC model provides a field reconstruction by determining both multipole coefficients of Eq. 4 and correction terms for both input and output TCs. Validation results for the theoretical 3D RFQ models are summarised in Table 2. Also here, the match is nearly perfect. All noisy and noiseless data points are represented with a maximum error of respectively 12 % and 0.2 %. Validation for the MYRRHA RFQ results in confidence intervals of maximum  $\pm 2.7\%$  without and maximum  $\pm 1.5\%$  with correction terms added to the surrogate model (Fig. 5). The correction terms enhance the mean  $\delta_{res,i}(z_{cell\ centre})$ , improving the potential approximation significantly along the cell.

## CONCLUSIONS

An accurate surrogate field model for an RFQ including RMs and TCs is implemented in the beam dynamics code

Table 2:  $\delta_{res,i}$  for the RM model and the TC model based on their identification collocation method for a noiseless and a noisy 3D potential data set.

Data set	Radial matcher $\delta_{res,i}$ [%]	Transition cell $\delta_{res,i}$
Noiseless	$-7.0e^{-12} < \delta_{res,i} < 5.8e^{-12}$	$-3.1e^{-11} < \delta_{res,i} < 4.8e^{-11}$
Noisy	$-7.7 < \delta_{res,i} < 6.6$	$-8.3 < \delta_{res,i} < 12.0$
Noiseless, noisy coeff. fit	$-0.3 < \delta_{res,i} < 0.2$	$-0.1 < \delta_{res,i} < 0.2$

V-Code and is validated against both theoretical models and the MYRRHA RFQ.

## REFERENCES

- [1] I.M. Kapchinskii, V.A. Teplyakov, *Linear ion accelerator with spacially homogeneous strong focusing*, Pribory i. Tekhnika Eksperimenta, 1970, vol. 119, pp. 19-22.
- [2] J.J. Manca, *Some new accelerating structures for high current intensity accelerators*, LA-7157-MS, LANL, 1978.
- [3] A. Schempp, *RFQ ion accelerators*, Nuclear Instruments and Methods in Physics Research Section B: Beam Interactions with Materials and Atoms, 1990, vol. 45, pp. 302-306
- [4] P. M. Bellan, *Fundamentals of plasma physics*, Cambridge University Press, 2006, pp. 609.
- [5] A. Wu Chao, M. Tigner *Handbook of accelerator physics and engineering*, World scientific, 2006, pp. 144-145.
- [6] W. Ackermann, T. Weiland, *Efficient time integration for beam dynamics simulations based on the moment method*, ICAP, 2006, pp. 208-211.
- [7] P.J. Channell *The moment approach to charged particle beam dynamics*, IEEE Transactions on Nuclear Science, 1983, pp. 2607-2609.
- [8] A. Novokhatski, T. Weiland, *Self-consistent model for the beams in accelerators*, ICAP, 1998, pp. 69-73.
- [9] V. Aseev, P. Ostroumov, E. Lessner, B. Mustapha, *Track: The new beam dynamics code*, PAC, 2005, pp. 2053-2055.
- [10] Computer Simulation Technology, CST STUDIO SUITE<sup>®</sup>, Bad Nauheimer Str. 19, D-64289 Darmstadt, Germany, <http://www.cst.com>, [Accessed: May 10, 2014].
- [11] J.W. Staples, *RFQs an introduction*, AIP, 1992, vol. 249, pp. 1483-1532
- [12] T.P. Wangler, *RF linear accelerators*, John Wiley & Sons, 2008, 2nd edition, pp. 232-281
- [13] K.R. Crandall, *RFQ radial matching sections and fringe fields*, LINAC84, 1984, GSI-84-11
- [14] B. Mustapha, A.A. Kolomiets, P.N. Ostroumov, *Full 3D Modeling of a Radio-Frequency-Quadrupole* LINAC10, 2010, pp. 542-544
- [15] T. Roggen, B. Masschaele, H. De Gerssem, W. Ackermann, S. Franke, T. Weiland, *Moment method beam dynamics code development: extended for radio frequency quadrupole simulations* IPAC13, 2013, pp. 879-881
- [16] MYRRHA Accelerator eXperiment (MAX), Available at: <http://ipnweb.in2p3.fr/MAX/index.php/> [Accessed: June 05 2014]